

Supporting information

Layer-by-layer printing of photopolymers in 3D: How weak is the interface?

H. Gojzewski^{1,2*}, Z. Guo³, W. Grzelachowska^{1,4}, M. G. Ridwan^{1,5}, M. A. Hempenius¹,
D.W. Grijpma³, G.J. Vancso^{1,6}

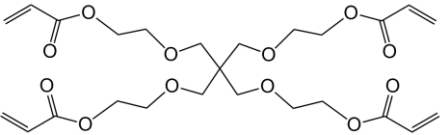
- 1) Materials Science and Technology of Polymers, Faculty of Science and Technology, University of Twente, Drienerlolaan 5, 7522 NB Enschede, The Netherlands
- 2) Faculty of Materials Engineering and Technical Physics, Poznan University of Technology, Piotrowo 3, 60-965 Poznan, Poland
- 3) Department of Biomaterials Science and Technology, Faculty of Science and Technology, University of Twente, Drienerlolaan 5, 7522 NB Enschede, The Netherlands
- 4) Faculty of Chemical Technology, Poznan University of Technology, Berdychowo 4, 60-965 Poznan, Poland
- 5) Petroleum Engineering Department, Bandung Institute of Technology, Jl. Ganeca No. 10 Bandung, 40135, Republic of Indonesia
- 6) School of Materials Science and Engineering, Nanyang Technological University, Singapore 639798, Singapore

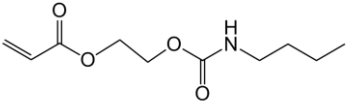
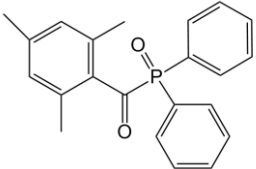
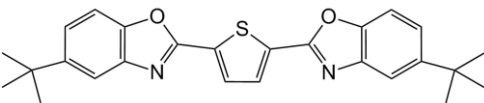
Corresponding author: h.gojzewski@utwente.nl

1. Chemical composition of the PR48 resin

The brand names, chemical names, chemical structures and wt/wt percentages of the Autodesk PR48 resin are shown in Table S1.¹

Table S1. Details of the resin PR48 composition.

Brand name	Chemical name	Chemical structure	wt/wt [%]
Sartomer 494 LM	Alkoxyated pentaerythritol tetraacrylate		39.776
Ebecryl 8210	-	unknown	39.776

Genomer 1122	2- [[[(Butylamino)carbonyl] oxy]ethyl acrylate		19.888
PL-TPO	2,4,6-Trimethylbenzoyl- diphenylphosphine oxide		0.400
OB plus	2,5-Bis(5- <i>tert</i> -butyl- benzoxazol-2-yl) thiophene		0.160

2. Differential scanning calorimetry

Samples for differential scanning calorimetry (DSC) analysis were prepared by adding PL-TPO initiator (0.4 wt%) (purchased from IGM Resins, the Netherlands) to the individual components of the PR48 resin, *i.e.* Sartomer 494 LM (15 mL) (Arkema, France), Ebecryl 8210 (15 mL) (Allnex, the Netherlands) and Genomer 1122 (15 mL) (Rahn, France), followed by stirring for 1 h. Ebecryl 8210 was additionally heated up to 80°C in order to homogenise the photoinitiator in the resin. The compositions were casted on a glass support and photopolymerized in a UV-crosslinking cabinet (Ultra-Lum UVC-508, USA) with UV wavelength 365 nm and light intensity 8 mW/cm² for 10 min under nitrogen atmosphere, in order to get highly cured resins.² As prepared samples were used to record DSC curves, along with the resin PR48 obtained by DLP-SLA.

Thermal characterization of individual polymer components of the resin PR 48 was conducted by DSC from –50 to 100°C, using a Perkin Elmer Pyris 1 DSC for specimens with a mass of 10–18 mg (Figure S1). Samples were subjected to two heating cycles (heating rate 30°C/min,

cooling rate 300°C/min). Traces recorded during the first and the second heating cycle were identical. The glass transition temperature (T_g) was evaluated during the first heating run as the midpoint of the transition.

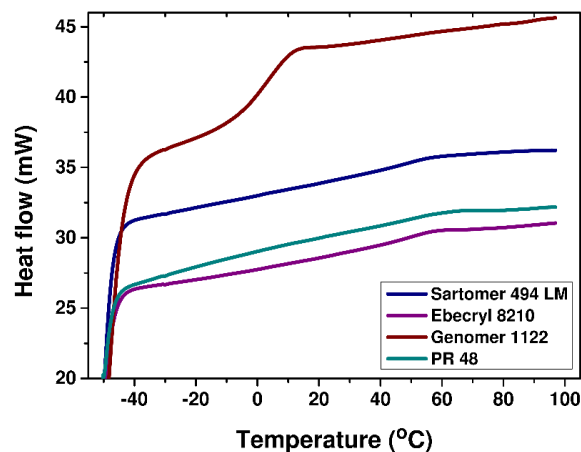


Figure S1. DSC traces obtained during the first heating run at a scan rate of 30 °C/min.

T_g values (midpoint) were 49.4, 46.4 and 3.5 °C for the photopolymerized Sartomer 494 LM, Ebecryl 8210 and Genomer 1122, respectively. We were not able to determine the T_g of the PR48 sample. Typically, with increasing crosslink density of a polymer, a broadening of the glass transition occurs, and the magnitude of the heat capacity change ΔC_p at T_g decreases, due to restricted main-chain motion caused by the crosslinks. In addition, network heterogeneities contribute to broadening of the glass transition. Therefore, it may be difficult, or even impossible, to detect glass transitions of highly crosslinked polymers by DSC.³⁻⁵

3. Spectroscopic analysis of Ebecryl 8210

In order to acquire chemical and structural information about the unknown resin PR48 component, i.e. Ebecryl 8210, a NMR and FTIR spectroscopies were conducted. A ^1H NMR spectrum of Ebecryl 8210 was recorded on a Bruker Avance III (400 MHz) instrument at 400.1 MHz in CDCl_3 (Figure S2). Spectrum indicates that this resin contains acrylate groups, as is

evident from resonances observed in the range of $\delta = 5.7\text{--}6.5$ ppm. Peaks found in the range of $\delta = 0.7\text{--}1.6$ ppm demonstrate the presence of aliphatic moieties, while no peaks in the aromatic region are observed.

A FTIR spectrum of the Ebecryl 8210 was recorded using a Bruker ALPHA spectrometer equipped with an ATR single reflection crystal (Bruker Optic GmbH) over the range of 4000 cm^{-1} to 400 cm^{-1} (Figure S3). Background spectra were recorded against air. The spectrum displays absorption bands typical of acrylate moieties at 1722 cm^{-1} (C=O stretch) and 1634 cm^{-1} (C=C stretch). In addition, an absorption band characteristic of hydroxyl groups ($3200\text{--}3650\text{ cm}^{-1}$) is present.

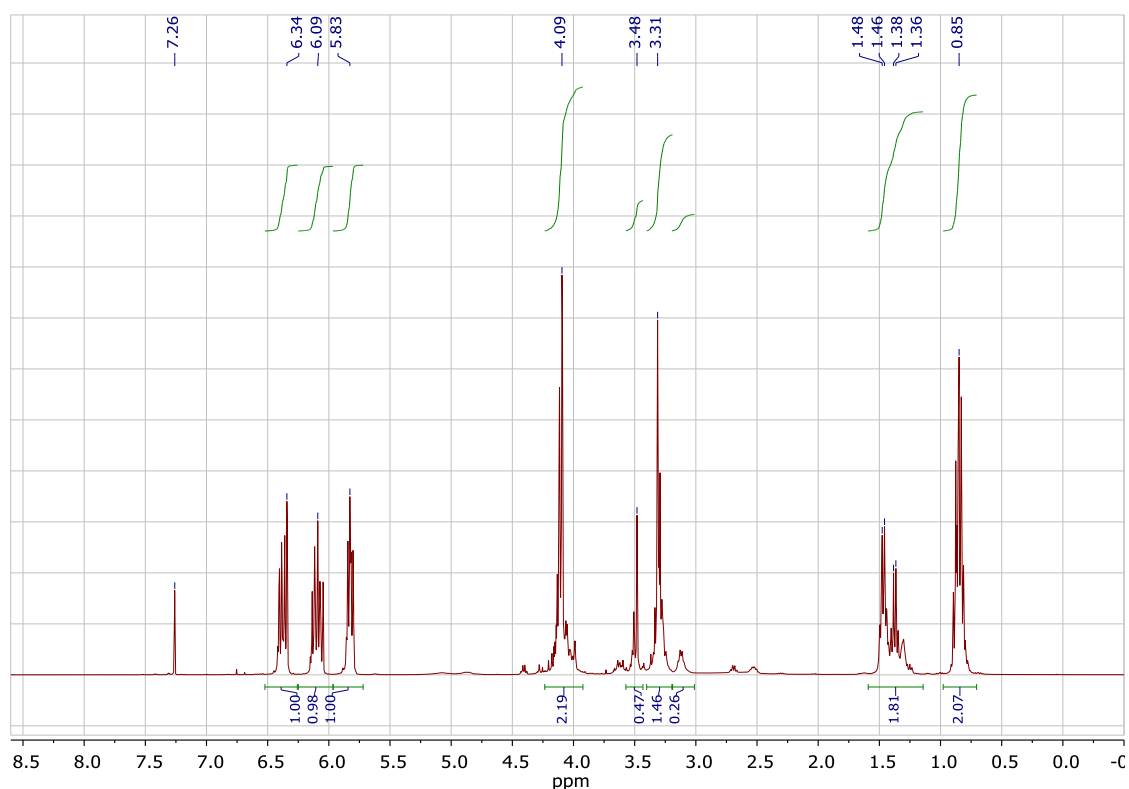


Figure S2. 400 MHz ^1H NMR spectrum of Ebecryl 8210, recorded in CDCl_3 .

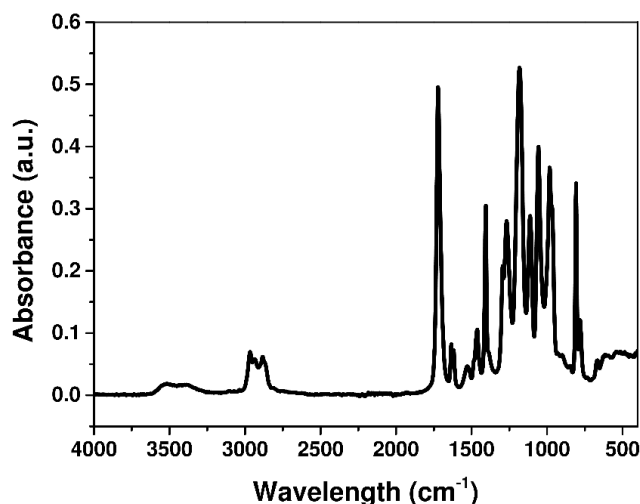


Figure S3. FTIR spectrum of Ebecryl 8210.

On the basis of these measurements it can be concluded that Ebecryl 8210 is an aliphatic resin possessing acrylate and hydroxyl functional groups. This is in agreement with the manufacturer's description which states that the resin is an aliphatic urethane acrylate with dual functionality (acrylate and primary hydroxyl groups). Due to the presence of primary hydroxyl groups, Ebecryl 8210 reacts with isocyanates.

4. Swelling

The swelling tests were performed to monitor potential cracking and failure of the polymer networks. Samples were immersed in five solvents, i.e. toluene, chloroform, isopropanol, tetrahydrofuran (THF), and acetone, for 10, 100 and 500 minutes, and imaged optically (Olympus BX60, Japan) immediately thereafter (Figure S4). The swelling test confirm the AFM analysis: within the interface the crosslinking density drops. The low-crosslinked polymer network swells, and the layers separate out, in a present of all organic solvents used, however, with different efficiency as related to the time of sample immersion.

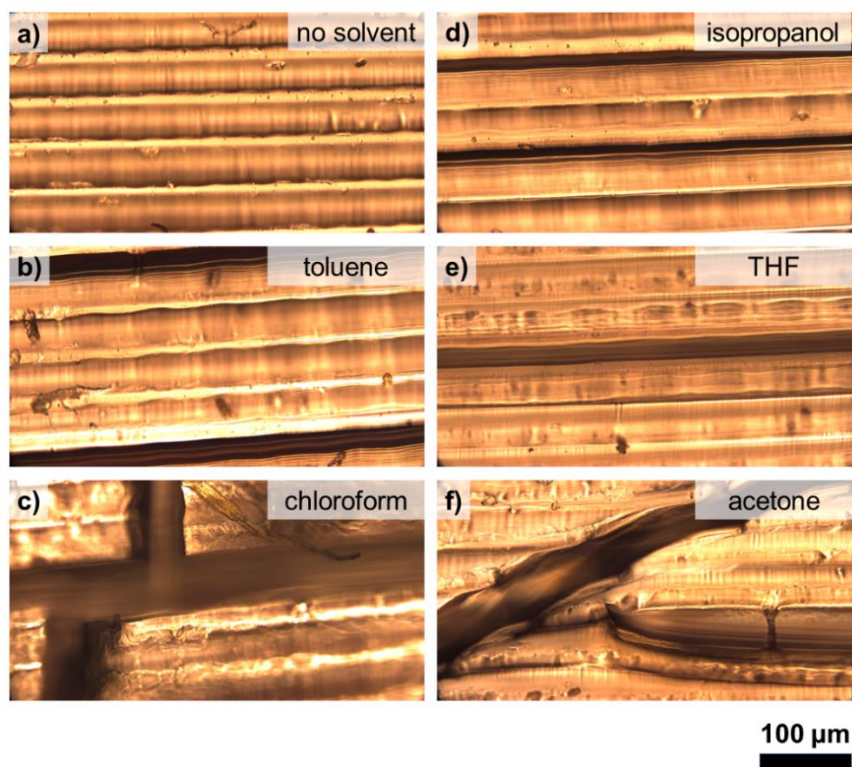


Figure S4. Optical images presenting a side-view of the DLP-SLA samples that were immersed in five solvents for 500 min, as indicated: (a) no solvent, (b) toluene, (c) chloroform, (d) isopropanol, (e) tetrahydrofuran, and (f) acetone.

The immersion time of 10 min results in no optical differences (nor swelling neither separation observed) at 50x magnification by optical microscopy. The immersion time of 100 min, however, is sufficient to delaminate layers when one uses chloroform and acetone. The delamination is caused by (intentional) mechanical dragging the sample. Swelling is minor. The immersion time of 500 min results in delamination of layers for all solvents used. Swelling is noticeable (near equilibrium). Chloroform and acetone penetrate the polymer network to a great extent, so that the samples can be easily broken even across the layering by mechanical manipulation.

5. Indentation depth maps (PF-QNM mode AFM)

To support the Figures 1f, 2a and 2b in the manuscript text, corresponding indentation depth maps are shown in Figure S5.

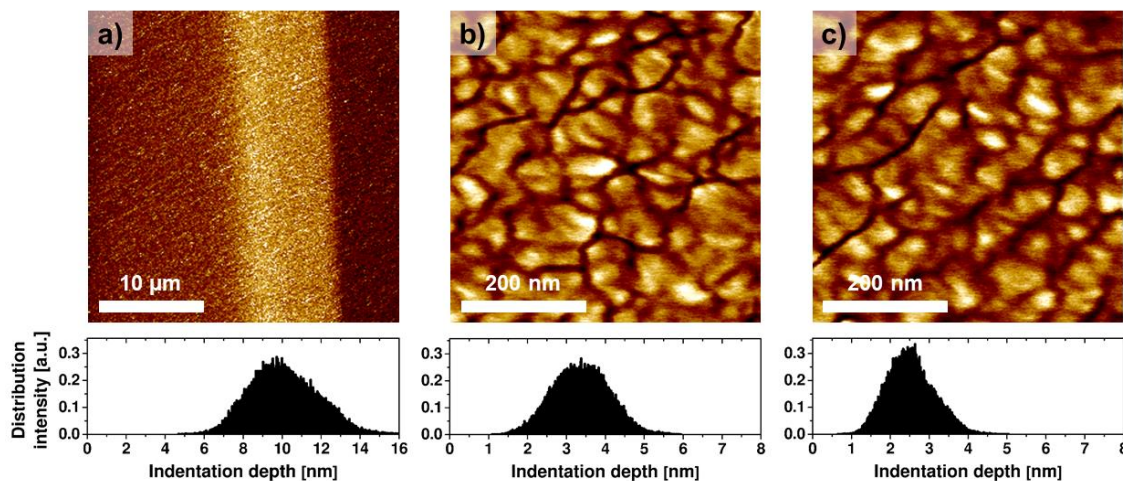


Figure S5. AFM indentation depth maps (a), (b) and (c) correspond to Figures 1f, 2a and 2b in the manuscript, respectively. The distributions of the indentation depth values per map are shown as histograms.

The presented distributions of the indentation depth values indicate the mechanical compliance over the interface (Figure S5a) and the urethane acrylate-based resin morphology at the submicron scale (Figure S5b-c).

6. Phase imaging (tapping mode AFM)

A Multimode 8 AFM retrofitted with a NanoScope V controller and a JV vertical engage scanner were used to collect phase images in tapping mode. As in case of PF-QNM imaging, data processing and data analysis were conducted with the NanoScope (ver. 8.15) and the NanoScope Analysis software (ver. 1.8), respectively. Measurements were performed in air, at controlled temperature (21 °C) and relative humidity (~ 40 %).

Tapping imaging is a basic AFM mode that allows one to obtain simultaneously topographic and phase images by recording the phase angle difference between the external excitation signal, that is driving the cantilever to oscillate.⁶ Heterogeneous specimens show a compositional contrast in phase images, which can be exposed by control and adjustment of ratio, r_{sp} , of the set point amplitude (A_{sp}) to the free oscillation amplitude (A_0) of the vibrating cantilever. The value of the set point amplitude refers to the amplitude of oscillation during imaging. We varied r_{sp} ratio from 0.58 to 0.40. Here, high-frequency (nominal 320 kHz) silicon cantilevers (model NCH, NanoWorld, Switzerland) were used with a nominal spring constant of 42 N/m and a nominal tip apex radius of 8 nm.

Figure S6a shows a perspective projection of the AFM phase image of the $60 \times 60 \mu\text{m}^2$ area. The interface is visible in bright color. The corresponding cross-section shows the phase-profile along the white line (Fig. S6b). The profile was smoothed by the Savitzky-Golay method (points of window: 30, polynomial order: 2).⁷ The largest phase contrast was observed at $r_{sp} = 0.4$.

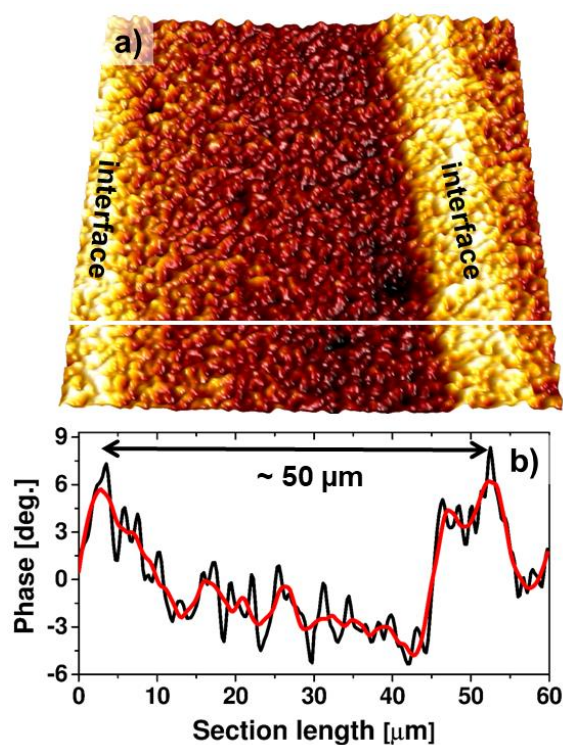


Figure S6. (a) AFM phase image (quasi-3D plot) of $60 \times 60 \mu\text{m}^2$ area, captured at $r_{sp} = 0.4$. (b) The cross-section is taken along the white line. The black arrow indicates the thickness of the layer. The profile is smoothed by the Savitzky-Golay method (red curve).

A visual inspection of the phase image shows that the phase angle reaches a maximum at the interface (see section plot at $\sim 3 \mu\text{m}$), decays significantly across the layer (from ~ 5 to $\sim 45 \mu\text{m}$), gets its minimum value before the consecutive interface is reached, and again - a maximum at the next interface ($\sim 53 \mu\text{m}$). The width of the interface is $10\text{-}14 \mu\text{m}$; a precise value is difficult to be obtained due to the presence of a diffuse domain boundary. Nevertheless, the bright area can be associated with energy dissipation dictated by the fact of lower cross-linking density at the interface.

7. Height images and cross-correlation analysis (PF-QNM mode AFM)

To ensure that there is a limited effect of the tip-surface tracking (height image creation) on the values in the Young's modulus and adhesion maps (presented in Figure 2 in the manuscript), we show the corresponding height images along with the cross-correlation analysis (Figure S7).

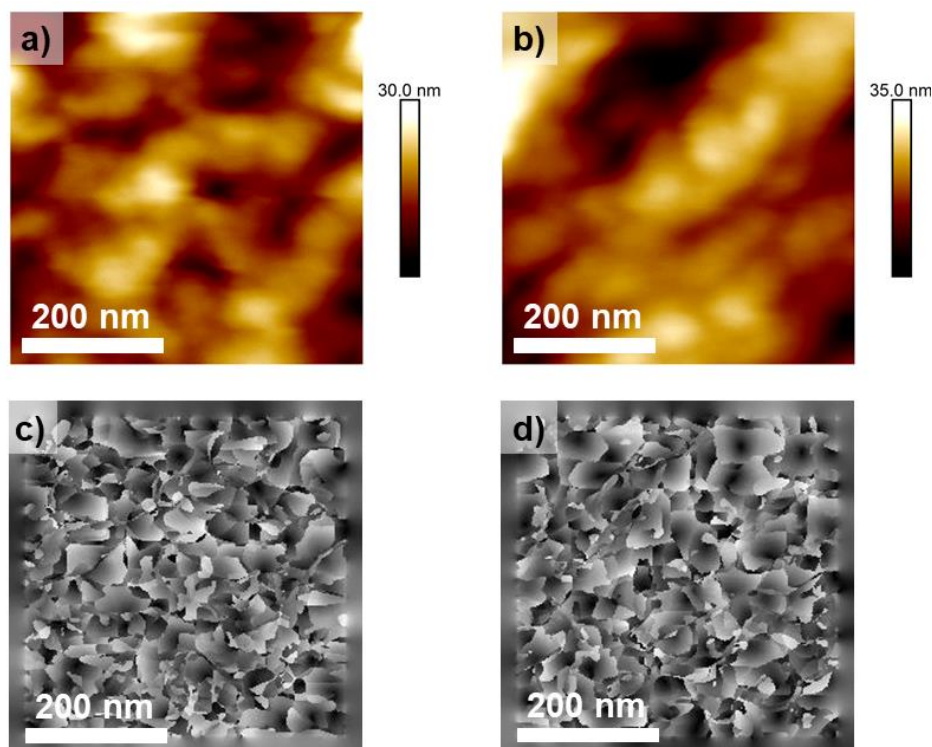


Figure S7. AFM height images (a) and (b) correspond to the images collected at the Location A and B, respectively, shown in Figures 2 in the manuscripts. The topographies were flattened using the 1st order polynomial function. Image (c) and (d) represent the absolute difference between the height images ((a) and (b)) and indentation depth maps shown in Figure S5b and S5c above, respectively. The blurred frames attached to (c) and (d) are due to the reduced window size (close to the image edges) of the algorithm used.

The cross-correlation analysis was performed in Gwyddion 2.55 software. The height images were correlated with the corresponding indentation depth maps to reveal their absolute difference within a window size of 20 pixels x 20 pixels. The result shows that the cross-

correlation images expose a non-ordered texture. The image texture is not related to specific features observed either in height images or in indentation depth maps. This can be translated to a very important point that the measured mechanical properties (Young's modulus, indentation depth and adhesion force) are not influenced by the changes of the tip vertical position (surface tracking) during scanning from one image pixel to another.

References

- (1) https://slidelegend.com/autodesk-standard-clear-prototyping-resin-pr48-discourse-cdn_5a1660de1723dd1e63e4c994.html (website access date: 21 Jan., 2020)
- (2) Bennett, J. Measuring UV Curing Parameters of Commercial Photopolymers Used in Additive Manufacturing *Addit. Manuf.* 2017, 18, 203-212.
- (3) Menczel, J.D.; Prime, R.B. *Thermal Analysis of Polymers: Fundamentals and Applications*, Wiley 2014.
- (4) Alves, N.M.; Ribelles, J.L.G.; Mano, J.F. Enthalpy Relaxation Studies in Polymethyl Methacrylate Networks with Different Crosslinking Degrees *Polymer* 2005, 46, 491-504.
- (5) Wu, Y.H.; Freeman, B.D. Structure, Water Sorption, and Transport Properties of Crosslinked N-Vinyl-2-Pyrrolidone/N,N'-Methylenebisacrylamide Films *J. Membr. Sci.* 2009, 344, 182-189.
- (6) García, R.; Pérez, R. Dynamic Atomic Force Microscopy Methods *Surf. Sci. Rep.* 2002, 47, 197-301.
- (7) Luo, J.; Ying, K.; Bai, J. Savitzky–Golay Smoothing and Differentiation Filter for Even Number Data *Signal Process.* 2005, 85, 1429-1434.